CVI
Journals.ASM.org

Evaluation of the Immunogenicity of *Mycobacterium bovis* BCG Delivered by Aerosol to the Lungs of Macaques

A. D. White, C. Sarfas, K. West, L. S. Sibley, A. S. Wareham, S. Clark, M. J. Dennis, A. Williams, P. D. Marsh, S. A. Sharpe

Public Health England, Microbiological Services Division, Porton Down, Salisbury, United Kingdom

Nine million cases of tuberculosis (TB) were reported in 2013, with a further 1.5 million deaths attributed to the disease. When delivered as an intradermal (i.d.) injection, the *Mycobacterium bovis* BCG vaccine provides limited protection, whereas aerosol delivery has been shown to enhance efficacy in experimental models. In this study, we used the rhesus macaque model to characterize the mucosal and systemic immune response induced by aerosol-delivered BCG vaccine. Aerosol delivery of BCG induced both Th1 and Th17 cytokine responses. Polyfunctional CD4 T cells were detected in bronchoalveolar lavage (BAL) fluid and peripheral blood mononuclear cells (PBMCs) 8 weeks following vaccination in a dose-dependent manner. A similar trend was seen in peripheral gamma interferon (IFN-γ) spot-forming units measured by enzyme-linked immunosorbent spot (ELISpot) assay and serum anti-purified protein derivative (PPD) IgG levels. CD8 T cells predominantly expressed cytokines individually, with pronounced tumor necrosis factor alpha (TNF-α) production by BAL fluid cells. T-cell memory phenotype analysis revealed that CD4 and CD8 populations isolated from BAL fluid samples were polarized toward an effector memory phenotype, whereas the frequencies of peripheral central memory T cells increased significantly and remained elevated following aerosol vaccination. Expression patterns of the α4β1 integrin lung homing markers remained consistently high on CD4 and CD8 T cells isolated from BAL fluid and varied on peripheral T cells. This characterization of aerosol BCG vaccination highlights features of the resulting mycobacterium-specific immune response that may contribute to the enhanced protection previously reported in aerosol BCG vaccination studies and will inform future studies involving vaccines delivered to the mucosal surfaces of the lung.

An estimated 9 million people contracted *Mycobacterium tuberculosis* in 2013, with a further 1.5 million deaths attributed to tuberculosis (TB) infection and coinfection with HIV (1). Vaccination is widely accepted to be the most effective method for control of an infectious disease. The current TB vaccine, *Mycobacterium bovis* BCG, is most commonly delivered as an intradermal (i.d.) injection. It is known to reduce the occurrence of disseminated forms of childhood TB (2) but displays variable efficacy against the infectious forms of adult pulmonary disease, suggesting that BCG-induced immunity may decline over time (3, 4). While several novel vaccines have progressed to clinical trials (5), none has yet improved upon the limited protection afforded by intradermal BCG vaccination. Typically, novel vaccines are delivered via a parenteral route, and, consequently, attention is now refocused on alternative routes for vaccine delivery, specifically aligning the route of vaccination with the natural route of TB infection using aerosol delivery methods (6–9). BCG has been shown to enhance protection against experimental *M. tuberculosis* infection when delivered intranasally or by aerosol to mice (10, 11) and as an aerosol to guinea pigs (12, 13) or rhesus macaques (14). However, the previous aerosol BCG immunization studies did not investigate in detail the immunological mechanisms underlying this protection.

A successful TB vaccine will need to induce persistent memory T-cell populations. There is an established division of labor between effector T cells (TEM) able to migrate to peripheral tissues through the expression of tissue-specific homing markers to execute inflammatory functions and central memory T cells (TCM) that reside within secondary lymphoid tissues ready to proliferate and replenish the TEM pool (15). The T-cell response to active TB infection has been shown to favor the TEM phenotype, with TCM more prevalent in latently infected individuals (16). Vaccine-induced TEM responses have been associated with protection against viral pathogens (17), and TEM populations have been investigated and detected following systemic BCG vaccination (18). Hence, it has been hypothesized that the current BCG vaccination induces TEM populations capable of the short-term control of *M. tuberculosis* infection but poorly induces the TCM populations required for long-term protection (19).

Currently there is no validated correlate of protection against *M. tuberculosis* infection, but a cell-mediated T-helper 1 (Th1) response from CD4 T cells (20) and probably a major histocompatability class (MHC) I restricted CD8 response (21) are known to be important for successful control of the disease. In the absence of a true correlate, functional markers such as gamma interferon (IFN-γ) expression are measured to assess vaccine immunogenicity. In recent years, the quality of the T-cell response has been highlighted as important to the induction of memory T cells (22), and multifunctional CD4 cells expressing combinations of

Received 13 May 2015 **Returned for modification** 5 June 2015
Accepted 23 June 2015

Accepted manuscript posted online 24 June 2015

Citation White AD, Sarfas C, West K, Sibley LS, Wareham AS, Clark S, Dennis MJ, Williams A, Marsh PD, Sharpe SA. 2015. Evaluation of the immunogenicity of *Mycobacterium bovis* BCG delivered by aerosol to the lungs of macaques. Clin Vaccine Immunol 22:992–1003. doi:10.1128/CVI.00289-15.

Editor: D. W. Pascual

Address correspondence to A. D. White, andrew.white@phe.gov.uk.

doi:10.1128/CVI.00289-15

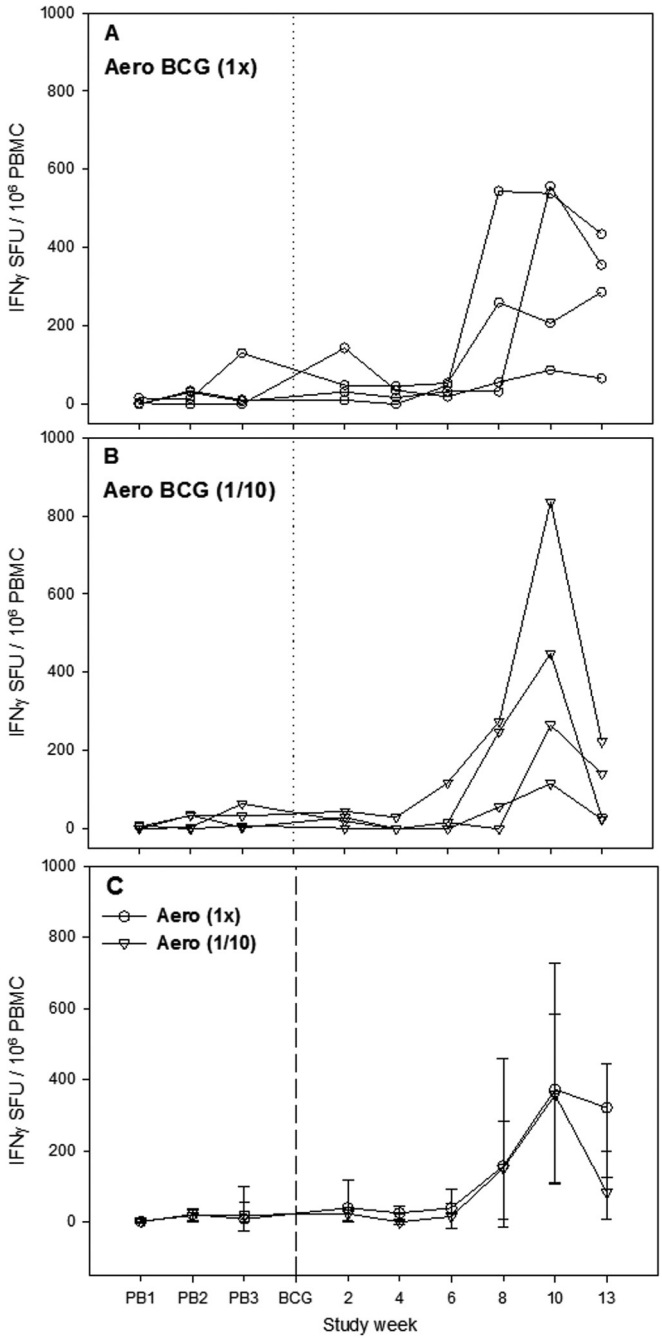

FIG 1 Frequencies of systemic PPD-specific IFN-γ spot-forming units (SFU) measured by ELISpot assay. The frequencies of PPD-specific IFN-γ SFU were measured in PBMCs following vaccination with aerosol-delivered BCG equivalent to a standard i.d. dose (Aero 1×) (A) and 10-fold less than a standard i.d. dose (Aero 1/10) (B). Panels A and B show SFU frequencies in individual animals, whereas panel C depicts vaccination group median SFU ± standard deviations. Vaccination with aerosol BCG is indicated by a dotted line at week zero.

the cytokines IFN-γ, tumor necrosis factor alpha (TNF-α), and interleukin-2 (IL-2) have been implicated both in the active phase of the disease (23) and as correlates of vaccine-induced protection (24–26). However, there is also evidence contradicting the legitimacy of these multifunctional cells as markers of anti-TB protective immunity (27), which highlights the likely complexity of the immune response required for tuberculosis immunity. Indeed, it is now clear that the CD4 T-helper response is diverse and includes cells of the Th17 lineage. IL-17 production has been implicated in the induction and maintenance of the Th1 response following BCG vaccination and recruitment of cells to the lung following infection with *M. tuberculosis* (28, 29) and correlates with improved outcome following *M. tuberculosis* exposure in nonhuman primates (NHP) (30).

The NHP model has many advantages over other species for the study of potential TB vaccines. These include the similarity of primate anatomy, physiology, susceptibility to low-dose aerosol infection, and, crucially, immune response to those of humans (31, 32). In this study, we used the rhesus macaque model to investigate mucosal and systemic immune responses induced following aerosol BCG vaccination. In doing so, we reveal features of the aerosol-induced immune response that may contribute to the enhanced protection reported in the literature and inform future vaccination strategies and the search for correlates of protection.

MATERIALS AND METHODS

Aerosolization of BCG and effect on vaccine viability. BCG was aerosolized by nebulization with the Omron MicroAIR device, and the effect of this on vaccine viability was investigated. One-milliliter solutions of BCG Danish strain 1331 (Statens Serum Institut [SSI], Copenhagen, Denmark) reconstituted in phosphate-buffered saline (PBS) were aerosolized through a sealed system to prevent loss of aerosol to the atmosphere, and cells were passively collected by condensation into sterile deionized water. The condensate was plated onto Middlebrook 7H11 selective agar containing oleic acid, bovine albumin, dextrose, and catalase (OADC) (bioMérieux, Basingstoke, United Kingdom) for enumeration of viable CFU. In parallel, CFU were measured in a nonaerosolized aliquot of identical BCG solution to enable quantification of any change in bacterial viability associated with the aerosolization process. To estimate the aerosol vaccination dose, losses associated with the nebulization apparatus and procedure were measured. BCG vaccine solution was nebulized through the Omron MicroAir device with an unsealed pediatric face mask, and the aerosol was collected in an all-glass impinger (AGI) (ACE Glass Inc., Vineland, NJ, USA) under conditions mimicking macaque inhalation and expiration. Viable CFU in collected aerosols were determined alongside those in nonaerosolized BCG solution as described above.

Experimental animals. Eight rhesus macaques (*Macaca mulatta*) of Indian origin aged between 4.6 and 5.2 years of age were obtained from an established United Kingdom breeding colony. The absence of a previous exposure to mycobacterial antigens was confirmed by tuberculin skin tests as part of the colony management procedures and by screening for IFN-γ enzyme-linked immunosorbent spot (ELISpot) assay (MabTech, Nacka, Sweden) responses to purified protein derivative (PPD) (SSI, Copenhagen, Denmark) and pooled 15-mer peptides of early secreted antigen target 6 (ESAT-6) and 10-kDa culture filtrate antigen (CFP-10) (Peptide Protein Research Ltd., Fareham, United Kingdom). Animals were housed in compatible social groups, in accordance with the Home Office (United Kingdom) Code of Practice for the Housing and Care of Animals Used in Scientific Procedures (1989) and the National Committee for Refinement, Reduction and Replacement (NC3Rs) Guidelines on Primate Accommodation, Care and Use, August 2006. For each procedure, sedation was applied by intramuscular injection with 10 mg ketamine hydrochloride (Ketaset; Fort Dodge Animal Health Ltd., Southampton, United Kingdom) per kilogram of body weight. All animal procedures were approved by the Public Health England Ethical Review Committee, Porton Down, United Kingdom, and authorized under an appropriate United Kingdom Home Office project license.

Vaccination. Sedated animals were exposed to aerosolized BCG Danish strain 1331 (SSI, Copenhagen, Denmark) using an Omron MicroAir mesh nebulizer (Omron Healthcare United Kingdom Ltd., Milton

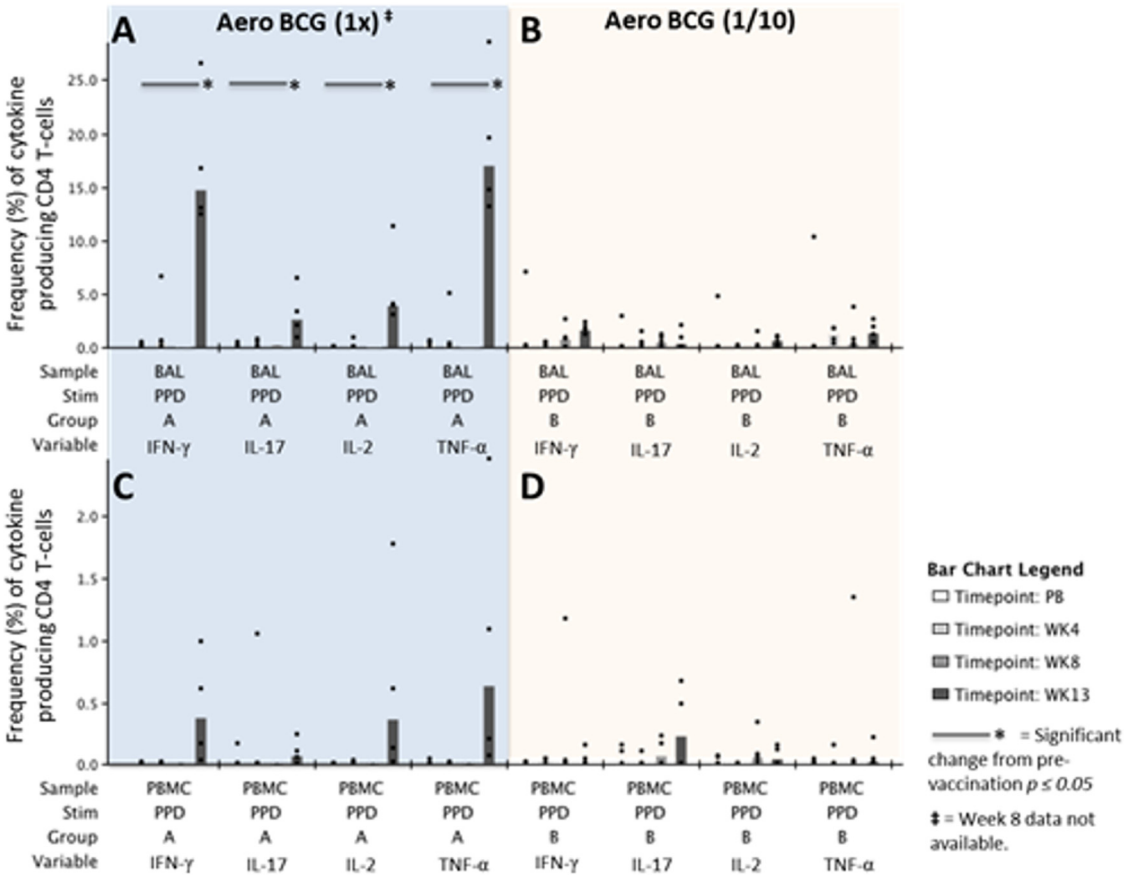

FIG 2 Aerosol BCG vaccination induces both Th1 and Th17 type cytokines in CD4 T cells isolated from BAL fluid (A, B) and peripheral blood (C, D). The bar charts display median values of the individual cytokines IFN-γ, TNF-α, IL-2, and IL-17 produced prior to vaccination (PB) and at weeks 4, 8, and 13 after aerosol BCG vaccination with a dose equivalent to (A, C) or 1/10 of (B, D) a standard i.d. dose. Cytokine frequencies in individual animals are represented by dots (n = 4 per vaccination group).

Keynes, United Kingdom) and a modified pediatric anesthesia mask. Vaccine doses were selected to be equivalent to or 1/10 of a standard adult intradermal dose after the expected losses in BCG titer associated with the aerosol delivery process were taken into account. BCG vaccine was prepared by adding 1 ml of PBS to each vaccine vial to give an estimated concentration of 2×10^6 to 8×10^6 CFU/ml. Multiple vials were pooled to ensure standardization between vaccinations, and 1/10 dose solutions were created by diluting this stock 1:10 with PBS before delivering 1 ml of the appropriate preparation to each animal.

Clinical assessment. Animals were sedated at two weekly intervals for blood sample collection and measurement of body weight and body temperature, red blood cell (RBC) hemoglobin levels, and erythrocyte sedimentation rates (ESR). RBC hemoglobin was measured using a HemoCue hemoglobinometer (HemoCue Ltd., Dronfield, United Kingdom), and the ESR was measured using the Sediplast system (Guest Medical, Edenbridge, United Kingdom). Animal behavior was observed throughout the study for contraindicators, including depression, withdrawal from the group, aggression, changes in feeding patterns, respiration rate, or coughing. Bronchoalveolar lavage (BAL) fluid was collected at 4-week intervals, as described previously (6).

Immune response analysis. (i) IFN-γ ELISpot assay. Gamma interferon (IFN-γ) ELISpot assays were performed on peripheral blood mononuclear cells isolated from heparin anticoagulated blood using standard methods, as previously described (6).

(ii) Intracellular cytokine staining. Intracellular cytokine staining (ICS) was performed on 1×10^6 BAL fluid cells or peripheral blood mononuclear cells (PBMCs) in medium (R10) consisting of RPMI 1640 supplemented with L-glutamine (2 mM), penicillin (50 U/ml), streptomycin (50 μg/ml), and 10% heat-inactivated fetal bovine serum. These cells were stimulated with a 10 μg/ml solution of CD28 and CD49d costimulatory antibodies (both from BD Biosciences, Oxford, United Kingdom) and 10 μg/ml PPD (SSI, Copenhagen, Denmark), 5 μg/ml staphylococcal enterotoxin B (SEB) (Sigma-Aldrich, Gillingham, United Kingdom), or R10 medium alone as a negative control. Intracellular cytokine staining to evaluate antigen-specific production of the cytokines IFN-γ, TNF-α, IL-2, and IL-17 was performed as previously described (6).

(iii) Immunophenotyping. Immunophenotyping was performed using 1×10^6 freshly isolated PBMCs or BAL fluid cells incubated for 30 min at room temperature with optimal dilutions of the following fluorescent antibodies: CD3-AF700, CD4-allophycocyanin (APC)-H7, CD8-fluorescein isothiocyanate (FITC), CD95 PeCy7, CCR7-phycoerythrin (PE), CD29-APC, and CD49d-BV711 (all from BD Biosciences, Oxford, United Kingdom), CD28-BV421 (BioLegend, London, United Kingdom), and CD14-ECD and CD20-ECD (Beckman Coulter, High Wycombe, United Kingdom). The amine-reactive Live/Dead fixable red dead cell stain kit was from Life Technologies (Renfrew, United Kingdom). BD CompBeads (BD Biosciences) were labeled with the above fluorochromes and used as compensation controls. Following antibody labeling, cells and beads were washed by centrifugation and fixed in 4% paraformaldehyde solution (Sigma-Aldrich, Gillingham, United Kingdom) prior to flow cytometric acquisition.

(iv) Flow cytometric acquisition and analysis. Cells were analyzed using a four-laser LSR II flow cytometer (BD Biosciences, Oxford, United Kingdom). Cytokine-secreting T cells were identified using a forward

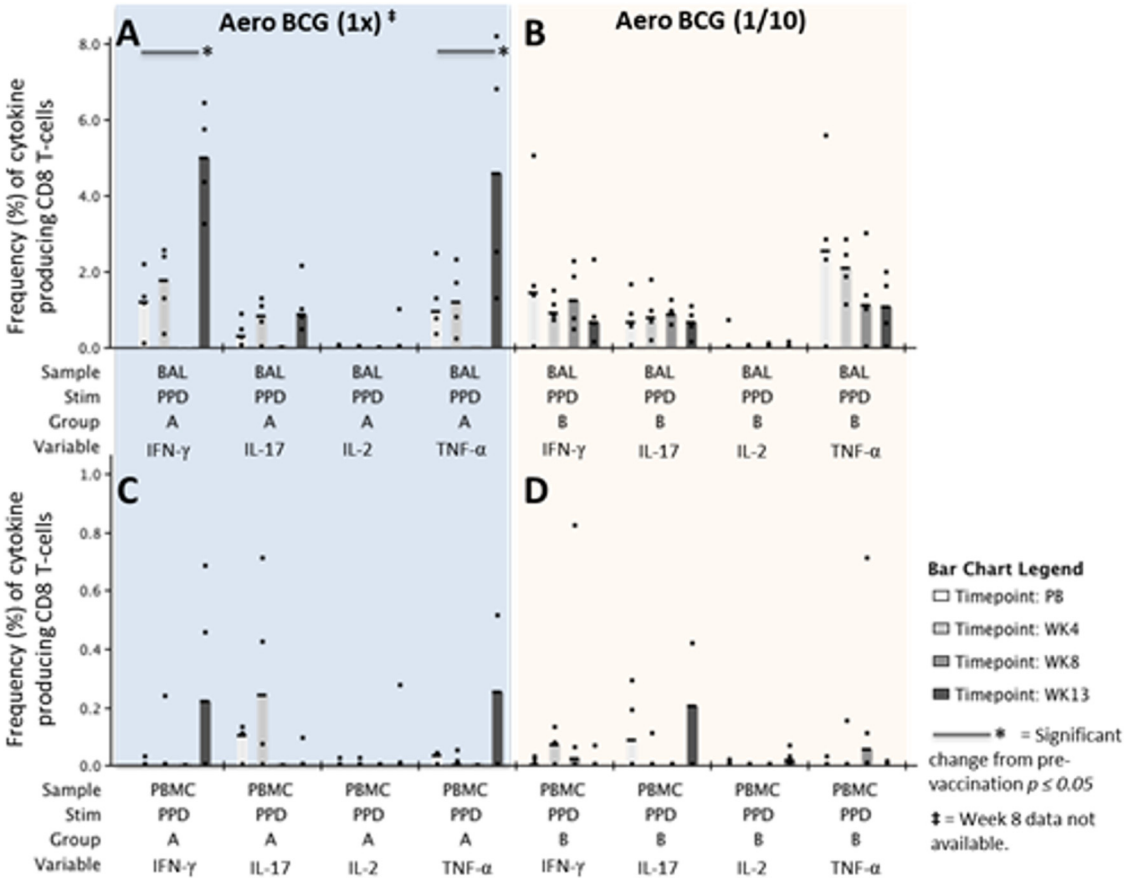

FIG 3 CD8 T-cell cytokine production in BAL fluid (A, B) and PBMCs (C, D) is indicative of an effector phenotype lacking IL-2 production. The bar charts display median values of the individual cytokines IFN-γ, TNF-α, IL-2, and IL-17 produced prior to vaccination (PB) and at weeks 4, 8, and 13 after aerosol BCG vaccination with a dose equivalent to (A, C) or 1/10 of (B, D) a standard i.d. dose. Cytokine frequencies in individual animals are represented by dots ($n = 4$ per vaccination group).

scatter height (FSC-H) versus side scatter area (SSC-A) dot plot to identify the lymphocyte population, to which appropriate gating strategies were applied to exclude doublet events, nonviable cells, monocytes ($CD14^+$), and B cells ($CD20^+$). For ICS analysis, sequential gating through $CD3^+$, $CD4^+$, and $CD8^-$ or $CD3^+$, $CD8^+$, and $CD4^-$ cells was used before individual cytokine gates to identify IFN-γ-, IL-2-, TNF-α-, and IL-17-producing subsets. For phenotyping analysis, CD4 and CD8 populations were identified using bivariate dot plots before assessment of homing marker expression using CD29 (β1 integrin chain) versus CD49d (α4 integrin chain) bivariate plots (see Fig. 8E and F). T-cell memory profiles were identified by gating on CD4 or CD8 populations with high surface staining for CD95, before differentiation of CD28 and CCR7 expression (see Fig. 6 and 7E to H). All data were analyzed using FlowJo (version 9.7.6; Tree Star, Ashland, OR, USA). Polyfunctional cells were identified using Boolean gating combinations of individual cytokine-producing CD4 or CD8 T cells. The software package PESTLE (version 1.7) was used for background subtraction to obtain antigen-specific ICS assay responses, and SPICE (version 5.35) was used to generate graphical representations of flow cytometry data (Mario Roederer, Vaccine Research Center, NIAID, NIH).

(v) Serum IgG ELISAs. Levels of anti-tuberculin PPD IgG in serum samples were measured by enzyme-linked immunosorbent assays (ELISAs). High protein binding capacity polystyrene plates (Fisher Scientific, Loughborough, United Kingdom) were coated with a 1 μg/ml solution of tuberculin PPD (SSI, Copenhagen, Denmark) suspended in pH 9.5 carbonate-bicarbonate buffer (Scientific Laboratory Supplies, Hessle, United Kingdom). Plates were washed and blocked using PBS plus 5% dried milk powder (BD Biosciences, Oxford, United Kingdom) before addition of 2-fold serial dilutions of serum samples. Following incubation, the plates were washed and incubated with 0.3 μg/ml goat anti-monkey IgG-horseradish peroxidase (HRP) (Insight Biotechnology Ltd., Wembley, United Kingdom). After further incubation and washing, the peroxidase substrate 3,3′,5,5′-tetramethylbenzidine (SurModics, Inc., Eden Prairie, MN, USA) was added to the wells, and the wells were incubated at room temperature for 10 min. The reaction was stopped by the addition of 2 M sulfuric acid (Fisher Scientific, Loughborough, United Kingdom), and the absorbance at 450 nm was measured immediately. Antibody titers were determined by linear regression of the sample dilution series and are expressed as arbitrary units relative to the mean pre-vaccination levels.

Necropsy. Before necropsy, animals were anesthetized with ketamine (15 mg/ml intramuscularly [i.m.]), weighed, and photographed, clinical data were collected, and exsanguination was performed via the heart, before termination by injection of a lethal dose of anesthetic (140 mg/kg Dolethal; Vétoquinol, Ltd., United Kingdom). A full necropsy was performed, and gross pathology was assessed. Samples of spleen, liver, kidneys, lymph nodes (hilar, inguinal, mesenteric, axillary, and colonic), tonsil, brain, olfactory bulb, heart and pericardium, small intestine (ileum, jejunum, and duodenum), transverse colon, eye, and the upper left lung lobe were removed, dissected on sterile trays, and placed into formalin-buffered saline for gross pathology and histopathology analysis.

Histopathology. Representative sections from the tissues described above were processed to paraffin wax, cut at 5 μm, and stained with hematoxylin and eosin (H&E) for microscopic examination. Pathology analysis was performed blinded to the vaccination dose and group.

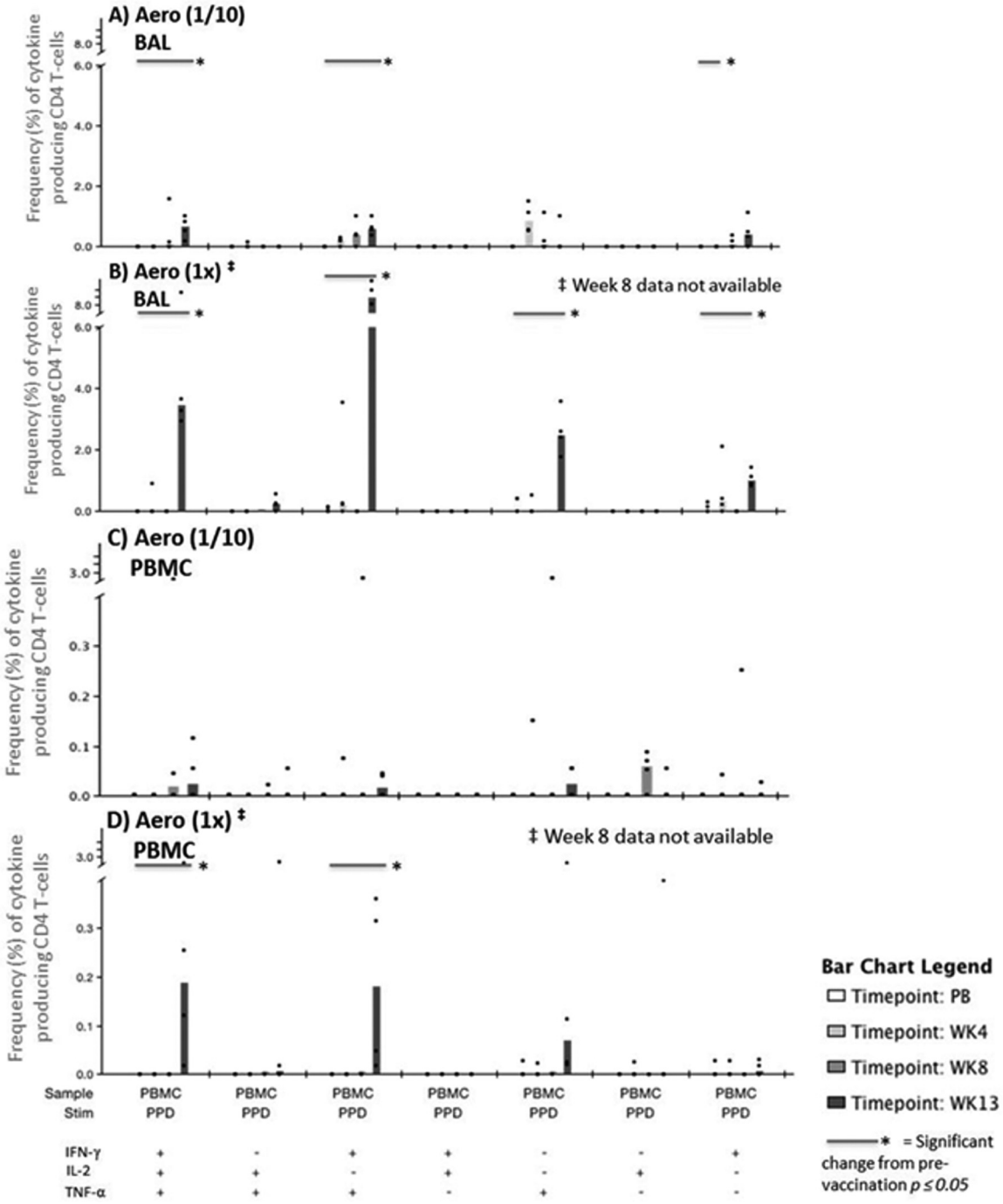

FIG 4 PPD-specific polyfunctional CD4 T-cell profiles measured in BAL fluid and PBMCs. The bar charts represent vaccination group median values for cytokine frequencies in BAL fluid (A, B) and PBMCs (C, D) prior to vaccination (PB) and at weeks 4, 8, and 13 after aerosol BCG vaccination with 1/10 of (A, C) or the equivalent of (B, D) a standard adult i.d. dose. Cytokine frequencies in individual animals are represented by dots ($n = 4$ per vaccination group).

Statistical analyses. Comparisons of *ex vivo* ELISpot assay responses and serum IgG titers were completed using the area under the curve (AUC) of each animal's response calculated using SigmaPlot version 10 (Systat Software Inc., Hounslow, United Kingdom). AUC values were compared between test groups using the nonparametric Mann-Whitney U test, Minitab version 15 (Minitab Ltd., Coventry, United Kingdom). To compare T-cell functional profiles measured by polyfunctional flow cytometry and T-cell homing and memory marker expression between vaccination groups, T-cell subset frequencies were compared using a Wilcoxon rank test at each analysis time point (SPICE version 5.35). Similarly, vaccine-induced changes in T-cell functional profiles and memory or homing marker expression within each vaccination group were assessed by comparing frequencies at each analysis time point with mean baseline values. Negative values in antigen-specific ICS data generated by background subtraction were replaced by a minimum threshold value (33).

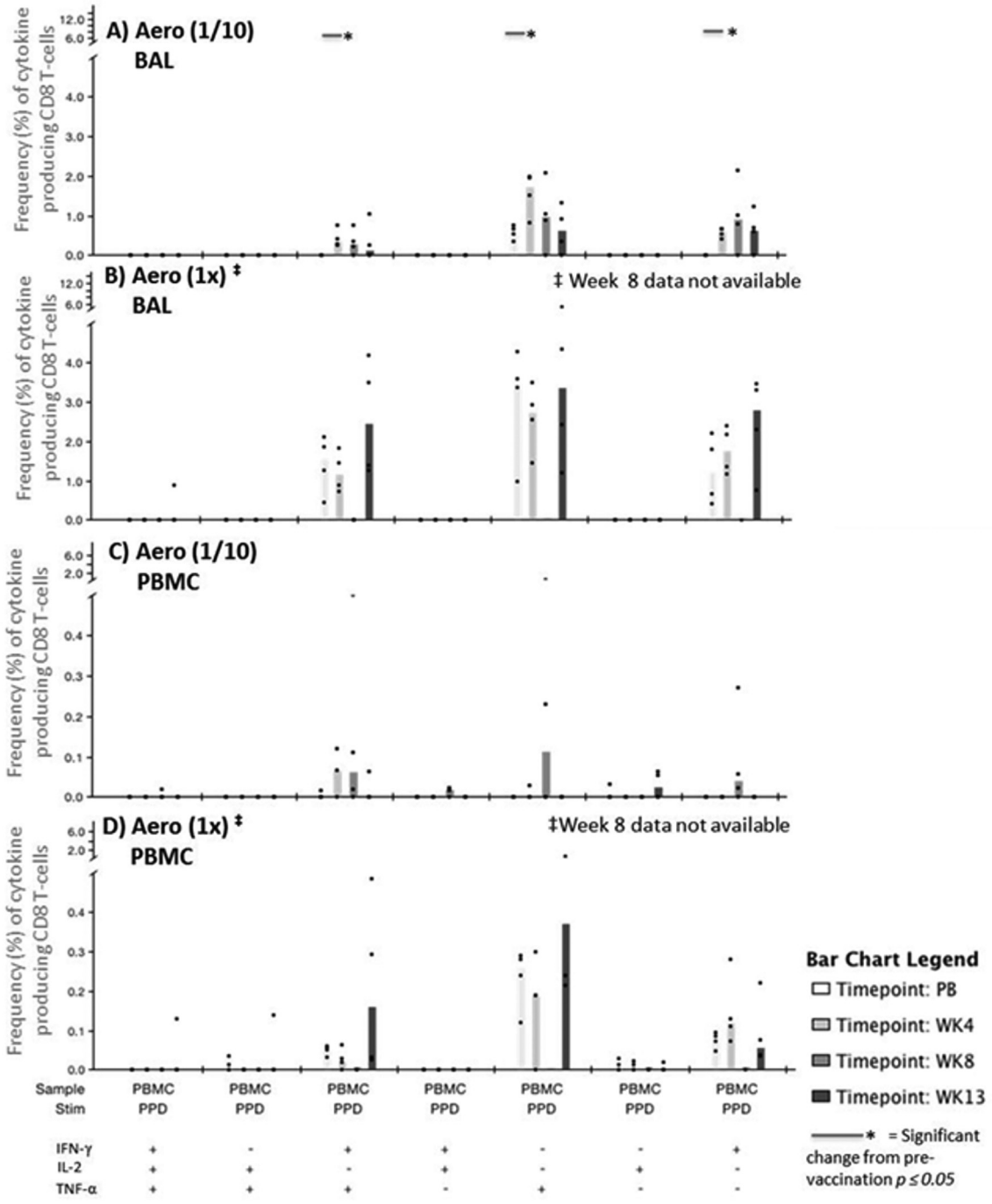

FIG 5 PPD-specific polyfunctional CD8 T-cell profiles measured in BAL fluid and PBMCs. The bar charts represent vaccination group median values for cytokine frequencies in BAL fluid (A, B) and PBMCs (C, D) prior to vaccination (PB) and at weeks 4, 8, and 13 after aerosol BCG vaccination with 1/10 of (A, C) or the equivalent of (B, D) a standard adult i.d. dose. Cytokine frequencies in individual animals are represented by dots ($n = 4$ per vaccination group).

RESULTS

BCG viability following aerosolization through the mesh nebulizer and determination of aerosol vaccine dose. The viability of BCG following aerosolization through a sealed system was confirmed by bacterial culture and comparison to nonaerosolized vaccine stock preparations. Stock solutions had viable counts of 4.4×10^5 CFU/ml, compared to mean counts of 3.15×10^5 CFU/ml $\pm$ 6.4×10^4 CFU/ml from passively collected aerosols. To estimate the aerosol vaccine dose, BCG was aerosolized through the unsealed nebulizer with a pediatric face mask and actively collected under conditions mimicking macaque respiration. Stock solutions of BCG had viable CFU counts of 5.35×10^5 CFU/ml, whereas the mean CFU collected from four repeat nebulizations of BCG solution was 4.49×10^4 CFU/ml $\pm$ 2.37×10^4 CFU/ml. This represented a 1.08-$\log_{10}$ reduction in viable BCG CFU/ml, implying that the aerosol BCG dose would

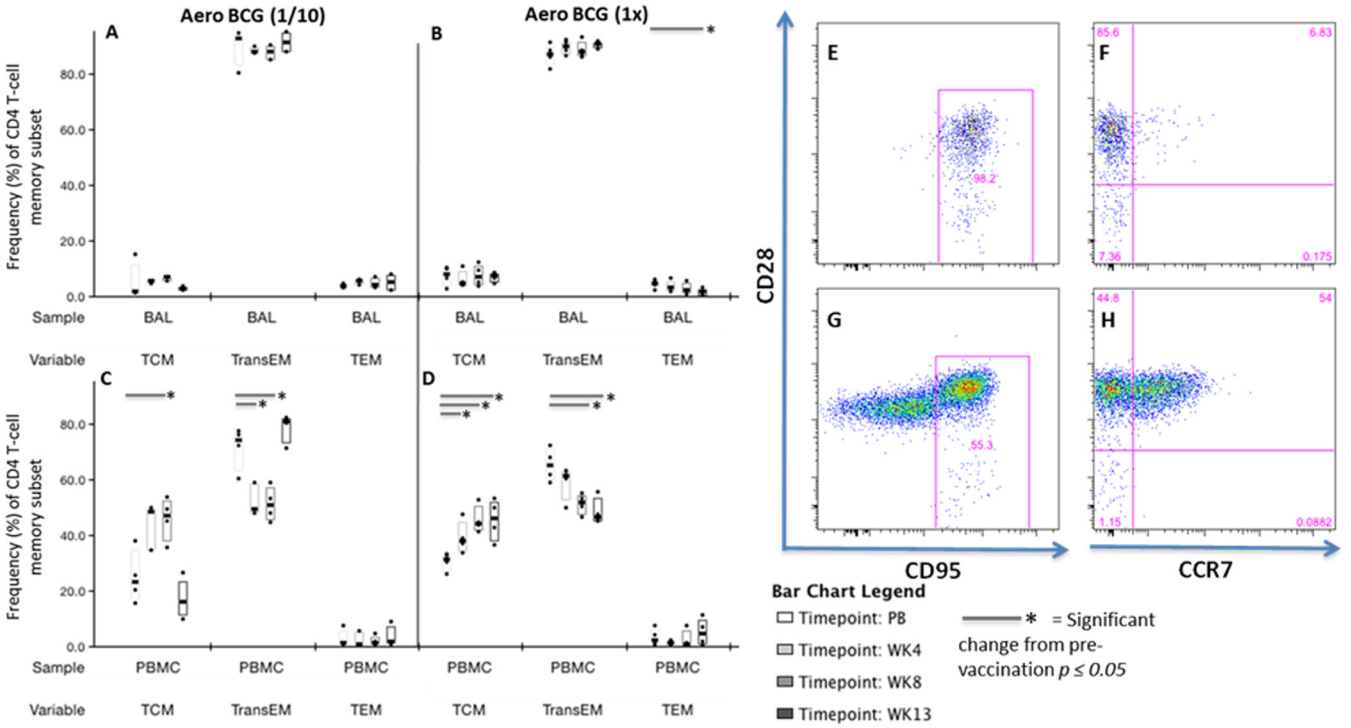

FIG 6 CD4 T cells isolated from BAL fluid samples remain polarized in an effector phenotype, whereas PBMC TCM populations expand following aerosol BCG vaccination. CD4 memory phenotype analysis of BAL fluid cells (A, B) and PBMCs (C, D) collected at baseline (PB) and at weeks 4, 8, and 13 after aerosol BCG vaccination with 1/10 of (A, C) or the equivalent of (B, D) a standard adult i.d. dose. The box plots show interquartile ranges (IQR) with medians represented as horizontal bars. Representative bivariate flow cytometry plots showing sequential gating of CD95-stained populations and definition of central to effector memory T-cell populations by patterns of CD28 and CCR7 expression in cells isolated from BAL fluid (E, F) and PBMCs (G, H).

be approximately 10-fold less than the titer of the nebulized BCG solution.

Safety of aerosol-delivered BCG. There were no observed perturbations beyond the normal ranges in body weight, temperature, peripheral lymph node size, red cell hemoglobin concentration, or erythrocyte sedimentation rate following aerosol BCG vaccinations.

Histopathology analysis by H&E staining of secondary lymphoid tissues did not reveal any adverse findings attributable to the BCG vaccination or route of administration.

The frequency of systemic PPD-specific IFN-γ-secreting cells increases following aerosol BCG vaccination. Systemic immune responses induced by aerosol BCG vaccination were profiled using an *ex vivo* IFN-γ ELISpot assay. Increases in PPD-specific IFN-γ spot-forming unit (SFU) frequencies were observed from 8 weeks after aerosol vaccination and reached significance at weeks 10 and 13 in both vaccination groups ($P = 0.03$) (Fig. 1). Significant differences were not detected between i.d.-equivalent and lower-dose aerosol vaccination groups when ELISpot assay AUCs measured across the study time course were compared by the Mann-Whitney U test ($P = 0.34$).

CD4 and CD8 T-cell responses measured by ICS are of Th1 and Th17 lineage following aerosol BCG vaccination. Antigen-specific production of the cytokines IFN-γ, TNF-α, IL-2, and IL-17 by CD4 and CD8 T cells was measured throughout the study by multiparameter ICS (Fig. 2 and 3). Cytokine production by CD4 and CD8 T cells in BAL fluid and PBMCs was characteristic of a Th1- and Th17-type response. A clear dose response was evident in both the mucosal and systemic T-cell populations, with significantly greater frequencies of IFN-γ-, IL-2-, and TNF-α-producing CD4 cells ($P = 0.02$) and IFN-γ-producing CD8 T cells ($P = 0.02$) detected in BAL fluid 13 weeks after aerosol BCG vaccination equivalent to a standard i.d. dose.

Peripheral and mucosal multifunctional T-cell response profiles induced by aerosol BCG vaccination. Mucosal and systemic polyfunctional profiles of CD4 and CD8 T cells producing combinations of the cytokines IFN-γ, IL-2, and TNF-α following aerosol BCG vaccination were measured throughout the study. CD4 responses induced by aerosol vaccination in BAL fluid cells were significantly above the prevaccination levels in four distinct profiles: IFN-γ, IL-2, and TNF-α triple-positive cells ($P = 0.02$), IFN-γ and TNF-α dual-positive cells ($P = 0.02$), and IFN-γ- or TNF-α-producing single-positive cells ($P = 0.02$) (Fig. 4A and B). A clear dose response was apparent between the vaccination groups in terms of mucosal CD4 T cells, with the frequency of triple-positive cells ($P = 0.02$), IFN-γ and TNF-α dual-positive cells ($P = 0.02$), and IFN-γ only-producing cells ($P = 0.02$) significantly greater following vaccination via the aerosol route with a dose equivalent to a standard i.d. vaccination. CD8 T cells in BAL fluid and PBMCs were found to produce IFN-γ or TNF-α or both cytokines simultaneously (Fig. 5A to D) and were present 4 weeks following aerosol vaccination. CD8 T cells producing TNF-α increased significantly in BAL fluid and were detected in PBMC samples following aerosol BCG vaccination.

Aerosol BCG vaccination leads to expansion of systemic central memory populations, whereas mucosal T cells remain polarized in an effector memory phenotype. Central and effector

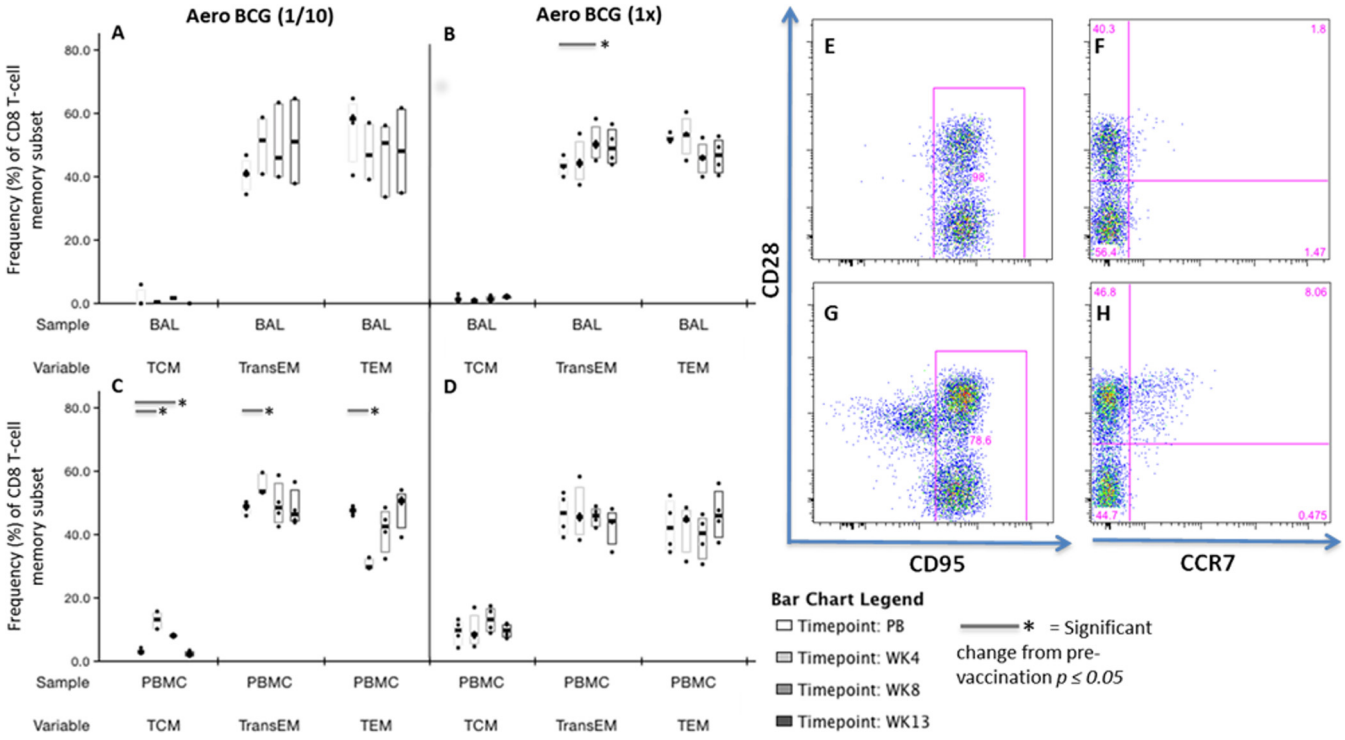

FIG 7 CD8 memory T-cell populations display a predominately effector memory phenotype split between the TransEM and TEM subsets. CD8 memory phenotype analysis applied to BAL fluid mononuclear cells (A, B) and PBMCs (C, D) collected at baseline (PB) and at weeks 4, 8, and 13 after aerosol BCG vaccination with 1/10 of (A, C) or the equivalent of (B, D) a standard adult i.d. dose. The box plots show IQR with medians represented as horizontal bars. Representative bivariate flow cytometry plots showing sequential gating of CD95-stained populations and definition of central to effector memory T-cell populations by patterns of CD28 and CCR7 expression in cells isolated from BAL fluid (E, F) and PBMCs (G, H).

memory T-cell populations are identified in the rhesus macaque by expression of cell activation markers such as CD95, followed by differential expression patterns of the costimulatory receptor CD28 and lymph node homing marker CCR7. Therefore, the central-to-effector memory axis was determined as $CD28^+$ $CCR7^+$ (TCM), $CD28^+$ $CCR7^-$ (transitional effector memory cells [TransEM]), and fully differentiated $CD28^-$ $CCR7^-$ (TEM) (Fig. 6E to H and 7E to H) (34, 35). Using this classification, T-cell memory profiles were assessed on cells isolated from BAL fluid and PBMCs at regular intervals throughout the study. CD4 and CD8 T cells from BAL fluid remained polarized in an effector T-cell phenotype throughout the study. CD4 T cells primarily occupied a TransEM profile; CD8 restricted cells were approximately evenly split between the TransEM and the fully differentiated TEM phenotype (Fig. 6A and B and 7A and B). A similar pattern was observed in CD4 and CD8 effector memory subsets isolated from peripheral blood but was accompanied by significant increases in TCM frequency. This TCM expansion was most pronounced in the CD4 subset and was seen in both aerosol vaccination groups. Expanded TCM populations remained elevated following aerosol BCG vaccination with a dose equivalent to the standard i.d. BCG vaccination, whereas the population had contracted and was significantly lower in the 1/10 dose group 13 weeks after vaccination ($P = 0.02$) (Fig. 6C and D and 7C and D).

α4β1 integrin homing markers are highly expressed by mucosal T cells. T-cell expression patterns of the α4 and β1 integrin chains were investigated as putative T-cell lung homing markers (Fig. 8). Dose-related differences in expression profiles were not observed following aerosol vaccination; therefore, data from the high- and lower-dose vaccination groups were combined for analysis purposes. The α4β1 integrin chains were highly expressed on CD4 and CD8 T cells isolated from BAL fluid prior to vaccination and remained consistently high throughout the study, with a significant increase in α4β1 coexpression on CD4 T cells 13 weeks following vaccination (Fig. 8A and C). The expression patterns on PBMCs were more varied and generally remained consistent throughout the study, although a trend for reduced α4β1 detection in the CD8 subset was noted 4 weeks after vaccination and was accompanied by a significant increase in the proportion of α4β1 double-negative cells at this time point (Fig. 8B and D).

Anti-tuberculin PPD IgG titers measured in serum increase following aerosol BCG vaccination. Levels of tuberculin PPD-specific IgG were measured in serum samples at selected time points throughout the study using a PPD ELISA. Median anti-PPD IgG titers increased in both vaccination groups relative to the prevaccination levels but had subsided 10 weeks later in the lower-dose vaccination group. Titers remained elevated in animals receiving aerosol vaccination equivalent to a standard i.d. dose (Fig. 9).

DISCUSSION

Despite a concerted global effort, TB remains a leading cause of mortality from an infectious agent. In recent years, the search for novel vaccines to improve upon the protection afforded by conventionally delivered BCG has begun to focus on alternative routes for vaccine delivery. Aerosol delivery of TB vaccines to the mucosal surface of the lung is a rational approach for localizing a

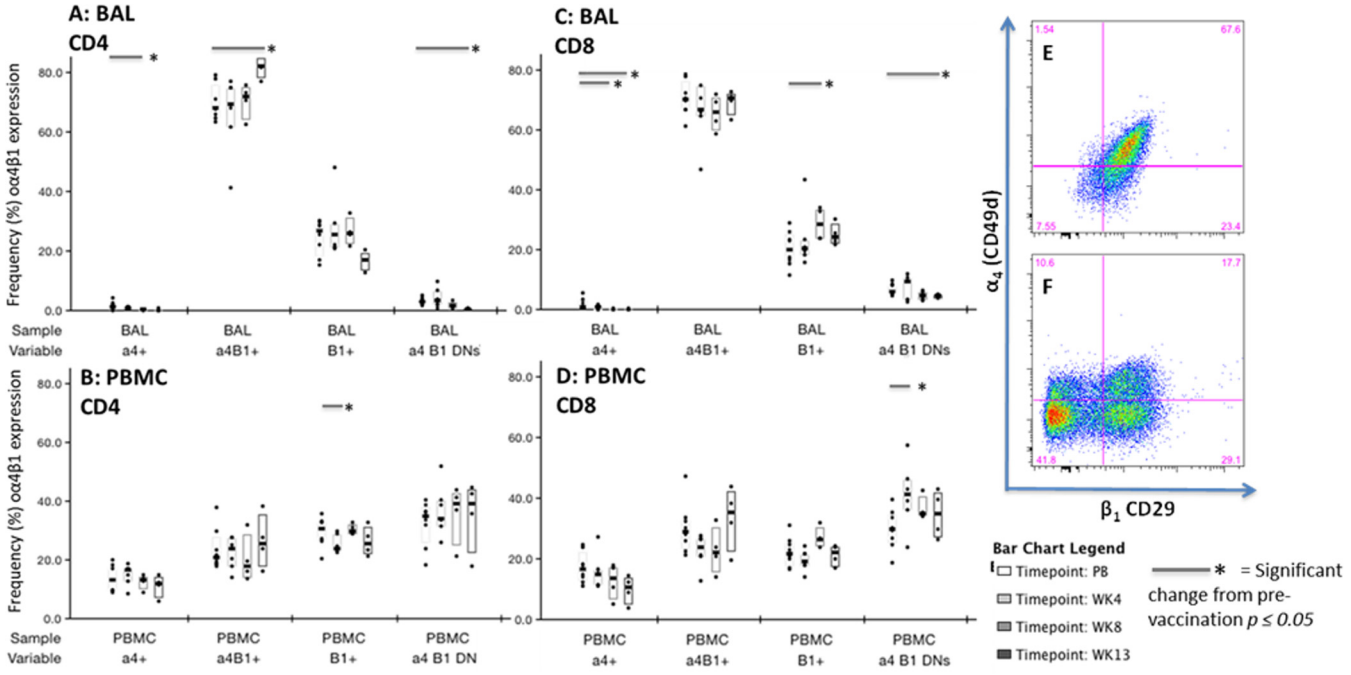

FIG 8 α4β1 integrins are expressed at high frequency by BAL fluid CD4 and CD8 T cells, whereas more varied expression is observed in PBMCs. Expression of the α4β1 integrin lung homing markers on CD4 and CD8 T cells was measured in cells isolated from BAL fluid (A, C) and PBMCs (B, D). The box plots show vaccination group medians and IQR of α4β1 integrin expression prior to vaccination (PB) and at weeks 4, 8, and 13 after aerosol BCG vaccination (standard i.d. dose equivalent and 1/10 dose vaccination groups combined). Patterns of homing marker expression on CD4 T cells isolated from BAL fluid are displayed in panel A and from PBMCs in panel B. Equivalent CD8 T-cell profiles are shown in panels C and D. Representative bivariate flow cytometry plots of α4 integrin (CD49d) and β1 integrin (CD29) chain staining on CD4 T cells isolated from BAL fluid (E) and PBMCs (F).

vaccine-induced response at the primary site of infection. Such an approach has proven practical and effective in the context of measles vaccination (36) and has recently proven safe and immunogenic in clinical trials of the novel TB vaccine MVA85A (7).

Aerosol-delivered BCG vaccination has previously been shown to afford enhanced protection against inhaled *M. tuberculosis* infection in the rhesus macaque (14). However, these studies did not describe the host response underpinning this protection. With this assessment of the immunogenicity of aerosol BCG vaccination, we highlight features of the mycobacterium-specific T-cell response induced via the mucosal vaccination route that may contribute to the enhanced protection observed in previous studies. Moreover, in comparison with recently published studies describing equivalent immunogenicity measures applied following i.d. BCG vaccination in age-matched rhesus macaques, a comparison can be drawn between the immune responses induced by each vaccination route (6). Multifunctional T-cell responses are thought to be an important component of a protective immune response against intracellular pathogens, including *M. tuberculosis* (24–26), and have been shown to be involved during the active phase of tuberculosis infection (23). Our results show that polyfunctional CD4 T cells are detected in the lung following aerosol vaccination and that the functional repertoire of CD4 and CD8 T cells induced by aerosol BCG was consistent with that reported in our prior studies of i.d. BCG immunogenicity. However, the frequency of antigen-specific cells was observed to increase at later time points following aerosol vaccination (6, 32). In addition, aerosol vaccination also induced TNF-α-secreting CD8 populations detectable at the mucosal surfaces or in the periphery. As antigen-specific TNF-α production has been implicated as a protective factor in the control of tuberculosis (37, 38) and anti-TNF-α therapy has been demonstrated to induce reactivation of latent infection (39, 40), this could prove to be an important factor in the protection imparted by aerosol BCG vaccination.

Delayed T-cell activation is an established phenomenon associated with *M. tuberculosis* infection and is often in contrast with the kinetics observed following infection with comparable intracellular pathogens and viruses (41–45). Our study suggests that the route of BCG vaccination has a significant impact on the kinetics of the cell-mediated response. This was seen as a delay in the peripheral response measured by the IFN-γ ELISpot assay, which was detected approximately 8 weeks following aerosol vaccination, whereas intradermally delivered BCG responses typically occur by week 4 (6, 32). Moreover, a similar trend was observed in CD4 T-cell cytokine production, including that of polyfunctional T cells, measured in BAL fluid and PBMCs, which was delayed relative to the cytokine production observed in prior i.d. BCG vaccination studies (6). This is also a notable retarding of T-cell induction relative to that observed following *M. tuberculosis* infection via the respiratory route, where PPD-specific IFN-γ SFU are usually detected within 4 weeks of infection in immunologically naive animals (32). Furthermore, such delayed activation of the mycobacterium-specific response may explain the protection observed in prior studies by Barclay et al. (14), as their study design delivered the *M. tuberculosis* challenge 8 weeks following vaccination, which would be during the peak of the primary aerosol BCG-induced vaccine response.

Induction of immunological memory is an essential feature of

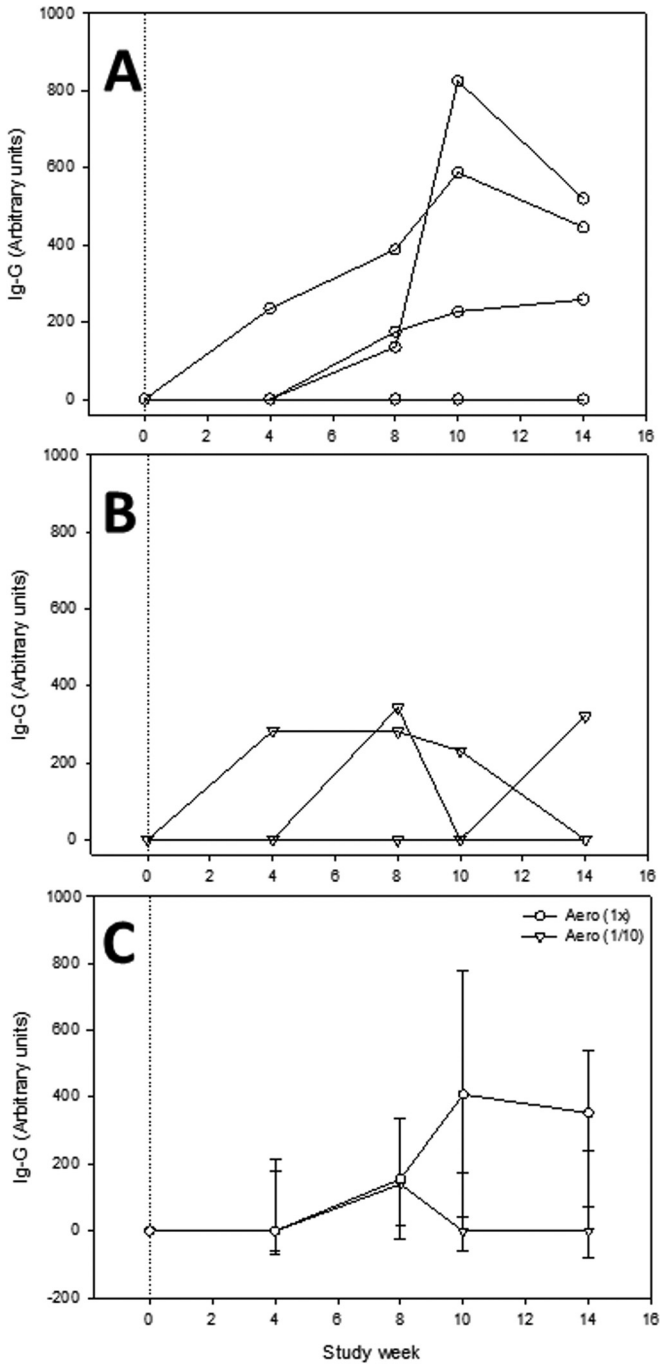

FIG 9 Increase in anti-tuberculin PPD IgG measured in serum following aerosol BCG vaccination. Anti-tuberculin PPD IgG titers measured in serum samples following vaccination with aerosol-delivered BCG equivalent to a standard adult i.d. dose (Aero 1×) (A) and 10-fold less than a standard adult i.d. dose (Aero 1/10) (B). IgG titers were established relative to the mean prevaccination levels (arbitrary units). Panels A and B show IgG titers measured in individual animals, whereas panel C depicts vaccination group median titers ± standard deviations. The vaccination with aerosol BCG is indicated by a dotted line at week zero.

a successful vaccine. BCG is primarily administered to infants or adolescents and confers protection against disseminated childhood forms of tuberculosis (2). However, the longevity of this protection is thought to wane beyond the adolescent years, suggesting that intradermally delivered BCG weakly induces long-lived memory T-cell responses (3, 4). Our T-cell memory phenotyping analysis shows that aerosol-delivered BCG leads to significant expansion of circulating CD4 central memory populations. This expansion persisted for at least 3 months following vaccination, after which point there was evidence for contraction of the TCM population in the lower-dose vaccination group. While different models exist to describe the development pathway of memory T-cell populations (46, 47), most agree that induction of the TCM subset leads to long-lived populations residing within secondary lymphoid tissues. However, we recognize that ours is a relatively short-term study and that longer time scales are required to assess the longevity of these cells beyond the primary phase of the vaccine response. Furthermore, measurement of functional markers such as cytokine production, cytotoxicity, and proliferation within the memory T-cell subsets is required to assess the antigen-specific recall capacity of these cells.

In agreement with previous observations, our data confirm that the T-cell repertoire within the lung is biased toward an effector phenotype (35, 48). This is further supported by the high levels of Th1 and Th17 effector cytokines we detected in cells isolated from BAL fluid. The homing capacity to peripheral organs is a key feature of TEM (47), and expression of the α4β1 integrin cell surface adhesion markers has been linked with T-cell enrichment in the lung (49) and lung localization of PPD-specific IFN-γ-producing CD4 cells in *M. tuberculosis*-infected patients (50). To investigate whether these markers could be used as correlates of mucosal immunity, we followed the surface expression dynamics of the α4β1 integrin chains following aerosol BCG vaccination. Our data confirm that CD4 and CD8 T cells isolated from BAL wash fluid coexpress α4β1 at a high level, supporting the use of these markers as a measure of lung homing capacity. However, expression frequencies remained unchanged in both BAL fluid and PBMC samples following vaccination. We believe this highlights the limitation of measuring global frequencies of these markers, which inevitably reduces an assay's sensitivity to detect small changes within the total T-cell pool. Therefore, characterization of homing marker expression on cells executing antigen-specific functions should be a priority for future studies.

Aerosol delivery of vaccines is a practical proposition in the clinical setting, holding many advantages over conventional needle-based approaches. The safety of delivering novel TB vaccines to rhesus macaques and healthy human volunteers has recently been established (6–9). However, despite the excellent safety record of BCG, particular caution is warranted in the context of delivering live, attenuated bacilli to the lung and nasopharyngeal surfaces. The primary objective of this study was to characterize the immunological profiles induced by aerosol BCG and contrast these with existing i.d. BCG immunogenicity data to elucidate potential correlates of mucosal immunity. In addition, we are able to report that aerosol BCG was well tolerated, with no contraindications observed in the clinical parameters measured. Moreover, histopathology analysis of secondary lymphoid tissues did not reveal any adverse findings attributable to the BCG vaccination or route of administration. However, further studies are required to demonstrate the safety of this approach before trials in human volunteers and immunocompromised individuals. Consequently, we intend to further investigate the efficacy of aerosol BCG vaccination and characterize the events following low-dose experimental *M. tuberculosis* infection to confirm the protection

reported in the literature and further interrogate correlates of mucosal immunity and protection.

ACKNOWLEDGMENTS

We thank the PHE Biological Investigations Group and NHP breeding colony staff for their expertise with animal procedures, Graham Hall and Emma Rayner for histopathological analysis of tissues, Laura Hunter for histology support, and Dominic Kelly for assistance with the assessment of BCG viability following aerosolization.

The views expressed here are those of the authors and not necessarily those of Public Health England.

REFERENCES

1. **Zumla A, George A, Sharma V, Herbert RHN, Baroness Masham of Ilton, Oxley A, Oliver M.** 2015. The WHO 2014 global tuberculosis report—further to go. Lancet Glob Health **3:**e10–e12. http://dx.doi.org/10.1016/S2214-109X(14)70361-4.
2. **Trunz BB, Fine P, Dye C.** 2006. Effect of BCG vaccination on childhood tuberculous meningitis and miliary tuberculosis worldwide: a meta-analysis and assessment of cost-effectiveness. Lancet **367:**1173–1180. http://dx.doi.org/10.1016/S0140-6736(06)68507-3.
3. **Colditz GA, Brewer TF, Berkey CS, Wilson ME, Burdick E, Fineberg HV, Mosteller F.** 1994. Efficacy of BCG vaccine in the prevention of tuberculosis. Meta-analysis of the published literature. JAMA **271:**698–702.
4. **Sterne JA, Rodrigues LC, Guedes IN.** 1998. Does the efficacy of BCG decline with time since vaccination? Int J Tuberc Lung Dis **2:**200–207.
5. **Kaufmann SHE, Lange C, Rao M, Balaji KN, Lotze M, Schito M, Zumla AI, Maeurer M.** 2014. Progress in tuberculosis vaccine development and host-directed therapies—a state of the art review. Lancet Respir Med **2:**301–320. http://dx.doi.org/10.1016/S2213-2600(14)70033-5.
6. **White AD, Sibley L, Dennis MJ, Gooch K, Betts G, Edwards N, Reyes-Sandoval A, Carroll MW, Williams A, Marsh PD, McShane H, Sharpe SA.** 2013. Evaluation of the safety and immunogenicity of a candidate tuberculosis vaccine, MVA85A, delivered by aerosol to the lungs of macaques. Clin Vaccine Immunol **20:**663–672. http://dx.doi.org/10.1128/CVI.00690-12.
7. **Satti I, Meyer J, Harris SA, Manjaly Thomas Z-R, Griffiths K, Antrobus RD, Rowland R, Ramon RL, Smith M, Sheehan S, Bettinson H, McShane H.** 2014. Safety and immunogenicity of a candidate tuberculosis vaccine MVA85A delivered by aerosol in BCG-vaccinated healthy adults: a phase 1, double-blind, randomised controlled trial. Lancet Infect Dis **14:**939–946. http://dx.doi.org/10.1016/S1473-3099(14)70845-X.
8. **Darrah PA, Bolton DL, Lackner AA, Kaushal D, Aye PP, Mehra S, Blanchard JL, Didier PJ, Roy CJ, Rao SS, Hokey DA, Scanga CA, Sizemore DR, Sadoff JC, Roederer M, Seder RA.** 2014. Aerosol vaccination with AERAS-402 elicits robust cellular immune responses in the lungs of rhesus macaques but fails to protect against high-dose *Mycobacterium tuberculosis* challenge. J Immunol **193:**1799–1811. http://dx.doi.org/10.4049/jimmunol.1400676.
9. **Hokey DA, Wachholder R, Darrah PA, Bolton DL, Barouch DH, Hill K, Dheenadhayalan V, Schwander S, Godin CS, Douoguih M, Pau MG, Seder RA, Roederer M, Sadoff JC, Sizemore D.** 2014. A nonhuman primate toxicology and immunogenicity study evaluating aerosol delivery of AERAS-402/Ad35 vaccine. Hum Vaccin Immunother **10:**2199–2210. http://dx.doi.org/10.4161/hv.29108.
10. **Chen L, Wang J, Zganiacz A, Xing Z.** 2004. Single intranasal mucosal *Mycobacterium bovis* BCG vaccination confers improved protection compared to subcutaneous vaccination against pulmonary tuberculosis. Infect Immun **72:**238–246. http://dx.doi.org/10.1128/IAI.72.1.238-246.2004.
11. **Nuermberger EL, Yoshimatsu T, Tyagi S, Bishai WR, Grosset JH.** 2004. Paucibacillary tuberculosis in mice after prior aerosol immunization with *Mycobacterium bovis* BCG. Infect Immun **72:**1065–1071. http://dx.doi.org/10.1128/IAI.72.2.1065-1071.2004.
12. **Gheorghiu M.** 1994. BCG-induced mucosal immune responses. Int J Immunopharmacol **16:**435–444. http://dx.doi.org/10.1016/0192-0561(94)90033-7.
13. **Garcia-Contreras L, Wong Y-L, Muttil P, Padilla D, Sadoff J, Derousse J, Germishuizen WA, Goonesekera S, Elbert K, Bloom BR, Miller R, Fourie PB, Hickey A, Edwards D.** 2008. Immunization by a bacterial aerosol. Proc Natl Acad Sci U S A **105:**4656–4660. http://dx.doi.org/10.1073/pnas.0800043105.
14. **Barclay WR, Busey WM, Dalgard DW, Good RC, Janicki BW, Kasik JE, Ribi E, Ulrich CE, Wolinsky E.** 1973. Protection of monkeys against airborne tuberculosis by aerosol vaccination with bacillus Calmette-Guerin. Am Rev Respir Dis **107:**351–358.
15. **Sallusto F, Lenig D, Förster R, Lipp M, Lanzavecchia A.** 1999. Two subsets of memory T lymphocytes with distinct homing potentials and effector functions. Nature **401:**708–712. http://dx.doi.org/10.1038/44385.
16. **Wang X, Cao Z, Jiang J, Niu H, Dong M, Tong A, Cheng X.** 2010. Association of mycobacterial antigen-specific $CD4^+$ memory T cell subsets with outcome of pulmonary tuberculosis. J Infect **60:**133–139. http://dx.doi.org/10.1016/j.jinf.2009.10.048.
17. **Hansen SG, Vieville C, Whizin N, Coyne-Johnson L, Siess DC, Drummond DD, Legasse AW, Axthelm MK, Oswald K, Trubey CM, Piatak M, Lifson JD, Nelson JA, Jarvis MA, Picker LJ.** 2009. Effector memory T cell responses are associated with protection of rhesus monkeys from mucosal simian immunodeficiency virus challenge. Nat Med **15:**293–299. http://dx.doi.org/10.1038/nm.1935.
18. **Kaveh DA, Bachy VS, Hewinson RG, Hogarth PJ.** 2011. Systemic BCG immunization induces persistent lung mucosal multifunctional CD4 TEM cells which expand following virulent mycobacterial challenge. PLoS One **6:**e21566. http://dx.doi.org/10.1371/journal.pone.0021566.
19. **Orme IM.** 2010. The Achilles heel of BCG. Tuberculosis (Edinb) **90:**329–332. http://dx.doi.org/10.1016/j.tube.2010.06.002.
20. **Chackerian AA, Perera TV, Behar SM.** 2001. Gamma interferon-producing $CD4^+$ T lymphocytes in the lung correlate with resistance to infection with *Mycobacterium tuberculosis*. Infect Immun **69:**2666–2674. http://dx.doi.org/10.1128/IAI.69.4.2666-2674.2001.
21. **Chen CY, Huang D, Wang RC, Shen L, Zeng G, Yao S, Shen Y, Halliday L, Fortman J, McAllister M, Estep J, Hunt R, Vasconcelos D, Du G, Porcelli SA, Larsen MH, Jacobs WR, Jr, Haynes BF, Letvin NL, Chen ZW.** 2009. A critical role for CD8 T cells in a nonhuman primate model of tuberculosis. PLoS Pathog **5:**e1000392. http://dx.doi.org/10.1371/journal.ppat.1000392.
22. **Seder RA, Darrah PA, Roederer M.** 2008. T-cell quality in memory and protection: implications for vaccine design. Nat Rev Immunol **8:**247–258. http://dx.doi.org/10.1038/nri2274.
23. **Caccamo N, Guggino G, Joosten SA, Gelsomino G, Di Carlo P, Titone L, Galati D, Bocchino M, Matarese A, Salerno A, Sanduzzi A, Franken WPJ, Ottenhoff THM, Dieli F.** 2010. Multifunctional $CD4^+$ T cells correlate with active *Mycobacterium tuberculosis* infection. Eur J Immunol **40:**2211–2220. http://dx.doi.org/10.1002/eji.201040455.
24. **Darrah PA, Patel DT, De Luca PM, Lindsay RWB, Davey DF, Flynn BJ, Hoff ST, Andersen P, Reed SG, Morris SL, Roederer M, Seder RA.** 2007. Multifunctional TH1 cells define a correlate of vaccine-mediated protection against *Leishmania major*. Nat Med **13:**843–850. http://dx.doi.org/10.1038/nm1592.
25. **Lindenstrøm T, Agger EM, Korsholm KS, Darrah PA, Aagaard C, Seder RA, Rosenkrands I, Andersen P.** 2009. Tuberculosis subunit vaccination provides long-term protective immunity characterized by multifunctional CD4 memory T cells. J Immunol **182:**8047–8055. http://dx.doi.org/10.4049/jimmunol.0801592.
26. **Aagaard C, Hoang TTKT, Izzo A, Billeskov R, Troudt J, Arnett K, Keyser A, Elvang T, Andersen P, Dietrich J.** 2009. Protection and polyfunctional T cells induced by Ag85B-TB10.4/IC31 against *Mycobacterium tuberculosis* is highly dependent on the antigen dose. PLoS One **4:**e5930. http://dx.doi.org/10.1371/journal.pone.0005930.
27. **Kagina BMN, Abel B, Scriba TJ, Hughes EJ, Keyser A, Soares A, Gamieldien H, Sidibana M, Hatherill M, Gelderbloem S, Mahomed H, Hawkridge A, Hussey G, Kaplan G, Hanekom WA, other members of the South African Tuberculosis Vaccine Initiative.** 2010. Specific T cell frequency and cytokine expression profile do not correlate with protection against tuberculosis after bacillus Calmette-Guérin vaccination of newborns. Am J Respir Crit Care Med **182:**1073–1079. http://dx.doi.org/10.1164/rccm.201003-0334OC.
28. **Khader SA, Bell GK, Pearl JE, Fountain JJ, Rangel-Moreno J, Cilley GE, Shen F, Eaton SM, Gaffen SL, Swain SL, Locksley RM, Haynes L, Randall TD, Cooper AM.** 2007. IL-23 and IL-17 in the establishment of protective pulmonary $CD4^+$ T cell responses after vaccination and during *Mycobacterium tuberculosis* challenge. Nat Immunol **8:**369–377. http://dx.doi.org/10.1038/ni1449.
29. **Gopal R, Lin Y, Obermajer N, Slight S, Nuthalapati N, Ahmed M,**

Kalinski P, Khader SA. 2012. Interleukin-23 dependent IL-17 drives Th1 responses following *Mycobacterium bovis* BCG vaccination. Eur J Immunol **42:**364–373. http://dx.doi.org/10.1002/eji.201141569.

30. **Wareham AS, Tree JA, Marsh PD, Butcher PD, Dennis M, Sharpe SA.** 2014. Evidence for a role for interleukin-17, Th17 cells and iron homeostasis in protective immunity against tuberculosis in cynomolgus macaques. PLoS One **9:**e88149. http://dx.doi.org/10.1371/journal.pone.0088149.
31. **Capuano SV, Croix DA, Pawar S, Zinovik A, Myers A, Lin PL, Bissel S, Fuhrman C, Klein E, Flynn JL.** 2003. Experimental *Mycobacterium tuberculosis* infection of cynomolgus macaques closely resembles the various manifestations of human *M. tuberculosis* infection. Infect Immun **71:**5831–5844. http://dx.doi.org/10.1128/IAI.71.10.5831-5844.2003.
32. **Sharpe SA, McShane H, Dennis MJ, Basaraba RJ, Gleeson F, Hall G, McIntyre A, Gooch K, Clark S, Beveridge NER, Nuth E, White A, Marriott A, Dowall S, Hill AVS, Williams A, Marsh PD.** 2010. Establishment of an aerosol challenge model of tuberculosis in rhesus macaques and an evaluation of endpoints for vaccine testing. Clin Vaccine Immunol **17:**1170–1182. http://dx.doi.org/10.1128/CVI.00079-10.
33. **Roederer M, Nozzi JL, Nason MC.** 2011. SPICE: exploration and analysis of post-cytometric complex multivariate datasets. Cytometry A **79:**167–174. http://dx.doi.org/10.1002/cyto.a.21015.
34. **Pitcher CJ, Hagen SI, Walker JM, Lum R, Mitchell BL, Maino VC, Axthelm MK, Picker LJ.** 2002. Development and homeostasis of T cell memory in rhesus macaque. J Immunol **168:**29–43. http://dx.doi.org/10.4049/jimmunol.168.1.29.
35. **Picker LJ, Reed-Inderbitzin EF, Hagen SI, Edgar JB, Hansen SG, Legasse A, Planer S, Piatak M, Lifson JD, Maino VC, Axthelm MK, Villinger F.** 2006. IL-15 induces $CD4^+$ effector memory T cell production and tissue emigration in nonhuman primates. J Clin Invest **116:**1514–1524. http://dx.doi.org/10.1172/JCI27564.
36. **Lin W-H, Griffin DE, Rota PA, Papania M, Cape SP, Bennett D, Quinn B, Sievers RE, Shermer C, Powell K, Adams RJ, Godin S, Winston S.** 2011. Successful respiratory immunization with dry powder live-attenuated measles virus vaccine in rhesus macaques. Proc Natl Acad Sci U S A **108:**2987–2992. http://dx.doi.org/10.1073/pnas.1017334108.
37. **Roach DR, Bean AGD, Demangel C, France MP, Briscoe H, Britton WJ.** 2002. TNF regulates chemokine induction essential for cell recruitment, granuloma formation, and clearance of mycobacterial infection. J Immunol **168:**4620–4627. http://dx.doi.org/10.4049/jimmunol.168.9.4620.
38. **Zganiacz A, Santosuosso M, Wang J, Yang T, Chen L, Anzulovic M, Alexander S, Gicquel B, Wan Y, Bramson J, Inman M, Xing Z.** 2004. TNF-α is a critical negative regulator of type 1 immune activation during intracellular bacterial infection. J Clin Invest **113:**401–413. http://dx.doi.org/10.1172/JCI18991.
39. **Bruns H, Meinken C, Schauenberg P, Härter G, Kern P, Modlin RL, Antoni C, Stenger S.** 2009. Anti-TNF immunotherapy reduces $CD8^+$ T cell–mediated antimicrobial activity against *Mycobacterium tuberculosis* in humans. J Clin Invest **119:**1167–1177. http://dx.doi.org/10.1172/JCI38482.
40. **Lin PL, Myers A, Smith L, Bigbee C, Bigbee M, Fuhrman C, Grieser H, Chiosea I, Voitenek NN, Capuano SV, Klein E, Flynn JL.** 2010. Tumor necrosis factor neutralization results in disseminated disease in acute and latent *Mycobacterium tuberculosis* infection with normal granuloma structure in a cynomolgus macaque model. Arthritis Rheum **62:**340–350. http://dx.doi.org/10.1002/art.27271.
41. **Chackerian AA, Alt JM, Perera TV, Dascher CC, Behar SM.** 2002. Dissemination of *Mycobacterium tuberculosis* is influenced by host factors and precedes the initiation of T-cell immunity. Infect Immun **70:**4501–4509. http://dx.doi.org/10.1128/IAI.70.8.4501-4509.2002.
42. **Cooper AM.** 2009. Cell-mediated immune responses in tuberculosis. Annu Rev Immunol **27:**393–422. http://dx.doi.org/10.1146/annurev.immunol.021908.132703.
43. **Reiley WW, Calayag MD, Wittmer ST, Huntington JL, Pearl JE, Fountain JJ, Martino CA, Roberts AD, Cooper AM, Winslow GM, Woodland DL.** 2008. ESAT-6-specific CD4 T cell responses to aerosol *Mycobacterium tuberculosis* infection are initiated in the mediastinal lymph nodes. Proc Natl Acad Sci U S A **105:**10961–10966. http://dx.doi.org/10.1073/pnas.0801496105.
44. **Wolf AJ, Desvignes L, Linas B, Banaiee N, Tamura T, Takatsu K, Ernst JD.** 2008. Initiation of the adaptive immune response to *Mycobacterium tuberculosis* depends on antigen production in the local lymph node, not the lungs. J Exp Med **205:**105–115. http://dx.doi.org/10.1084/jem.20071367.
45. **Shaler CR, Horvath C, Lai R, Xing Z.** 2012. Understanding delayed T-cell priming, lung recruitment, and airway luminal T-cell responses in host defense against pulmonary tuberculosis. Clin Dev Immunol **2012:**628293. http://dx.doi.org/10.1155/2012/628293.
46. **Harrington LE, Janowski KM, Oliver JR, Zajac AJ, Weaver CT.** 2008. Memory CD4 T cells emerge from effector T-cell progenitors. Nature **452:**356–360. http://dx.doi.org/10.1038/nature06672.
47. **Mahnke YD, Brodie TM, Sallusto F, Roederer M, Lugli E.** 2013. The who's who of T-cell differentiation: human memory T-cell subsets. Eur J Immunol **43:**2797–2809. http://dx.doi.org/10.1002/eji.201343751.
48. **Henao-Tamayo MI, Ordway DJ, Irwin SM, Shang S, Shanley C, Orme IM.** 2010. Phenotypic definition of effector and memory T-lymphocyte subsets in mice chronically infected with *Mycobacterium tuberculosis*. Clin Vaccine Immunol **17:**618–625. http://dx.doi.org/10.1128/CVI.00368-09.
49. **Feng CG, Britton WJ, Palendira U, Groat NL, Briscoe H, Bean AG.** 2000. Up-regulation of VCAM-1 and differential expansion of beta integrin-expressing T lymphocytes are associated with immunity to pulmonary *Mycobacterium tuberculosis* infection. J Immunol **164:**4853–4860. http://dx.doi.org/10.4049/jimmunol.164.9.4853.
50. **Walrath JR, Silver RF.** 2011. The α4β1 integrin in localization of *Mycobacterium tuberculosis*-specific T helper type 1 cells to the human lung. Am J Respir Cell Mol Biol **45:**24–30. http://dx.doi.org/10.1165/rcmb.2010-0241OC.